Two-Electron Reactions $S_2Q_B \rightarrow S_0Q_B$ and $S_3Q_B \rightarrow S_1Q_B$ are Involved in Deactivation of Higher S States of the Oxygen-Evolving Complex of Photosystem II

Taras K. Antal, Päivi Sarvikas, and Esa Tyystjärvi*
Department of Biology, University of Turku, FI-20014 Turku, Finland

ABSTRACT The oxygen-evolving complex of Photosystem II cycles through five oxidation states (S_0–S_4), and dark incubation leads to 25% S_0 and 75% S_1. This distribution cannot be reached with charge recombination reactions between the higher S states and the electron acceptor Q_B^-. We measured flash-induced oxygen evolution to understand how S_3 and S_2 are converted to lower S states when the electron required to reduce the manganese cluster does not come from Q_B^-. Thylakoid samples preconditioned to make the concentration of the S_1 state 100% and to oxidize tyrosine Y_D were illuminated by one or two laser preflashes, and flash-induced oxygen evolution sequences were recorded at various time intervals after the preflashes. The distribution of the S states was calculated from the flash-induced oxygen evolution pattern using an extended Kok model. The results suggest that S_2 and S_3 are converted to lower S states via recombination from $S_2Q_B^-$ and $S_3Q_B^-$ and by a slow change of the state of oxygen-evolving complex from S_3 and S_2 to S_1 and S_0 in reactions with unspecified electron donors. The slow pathway appears to contain two-electron routes, $S_2Q_B \rightarrow S_0Q_B$, and $S_3Q_B \rightarrow S_1Q_B$. The two-electron reactions dominate in intact thylakoid preparations in the absence of chemical additives. The two-electron reaction was replaced by a one-electron-per-step pathway, $S_3Q_B \rightarrow S_2Q_B \rightarrow S_1Q_B$ in PS II-enriched membrane fragments and in thylakoids measured in the presence of artificial electron acceptors. A catalase effect suggested that H_2O_2 acts as an electron donor for the reaction $S_2Q_B \rightarrow S_0Q_B$ but added H_2O_2 did not enhance this reaction.

INTRODUCTION

The oxidation of water to molecular oxygen takes place in the oxygen-evolving complex (OEC), a functional part of Photosystem II (PS II) (1,2). OEC consists of an Mn_4O_4Ca cluster, its ligands, and tyrosine Y_Z of polypeptide D_1 (3–5). The light-induced charge separation in the reaction center of PS II generates the strongly oxidizing cation radical $P_{680}^{+\bullet}$ that oxidizes the manganese complex via Y_Z. To split water, OEC accumulates four positive equivalents, cycling successively through the redox states denoted S_0, S_1, S_2, S_3, and S_4, where S_0 and S_4 are the most reduced and the most oxidized state, respectively (6). The S_4 state is unstable and decays rapidly into the S_0 state, and the liberation of oxygen occurs during the S_3-S_4-S_0 transition.

Flash-induced oxygen evolution shows a damped period four oscillation on illumination of PS II with a train of short saturating flashes (6,7). The damping occurs because electron transfer from manganese to Q_B is not completed in some reaction centers after a saturating flash (miss) and because one flash can induce two cycles of electron transfer reactions (double hit) (6,8). Distribution of the S states of OEC can be evaluated from the flash-induced oxygen evolution sequence by using a model introduced by Kok et al. (6), assuming that the miss probability is equal for all S states. An alternative model with unequal miss probabilities has been proposed, and also this model showed a good fit to experimental data (9,10). A special case of models with unequal miss probabilities is a model in which misses can occur only during one S state transition whereas the other S state transitions occur without misses (9). We will call this a one-miss model.

During dark adaptation of several minutes, all higher S states deactivate to the S_1 state that is stable in the dark (7). S_2 and S_3 states can be reduced in ~30 s by charge recombination reactions with the quinone electron acceptor Q_B^- and by a fast (a few seconds) but minor pathway in which tyrosine Y_D^{red} of polypeptide D_2 acts as an electron donor (11–13). In addition, cytochrome b_{559} has been proposed to be an electron donor to the higher S states (14,15). When the acceptor side of PS II, including Q_B, is oxidized, the decay half time of the higher S states increases three- to fourfold (16). Styring and Rutherford (17) examined the deactivation of higher S states in PS II enriched membranes in which both Y_D and the PS II acceptor side were oxidized. Under these circumstances, higher S states deactivated slowly in 3–4 min, and S_3 decayed in a one-electron-per-step pathway via S_2. However, some electron acceptors like parabenzoquinone (PPBQ) used in Styring and Rutherford (17) to oxidize the PS II acceptor side, have been shown to destabilize the deactivation process of OEC (18,19). In measurements from PS II enriched membranes in the absence of electron acceptors, the decay of the S_2 state seemed to be independent of the decay of the S_3 state (20). There are no earlier thorough studies of the slow deactivation mechanism in thylakoid membranes or in other preparations in the absence of artificial electron acceptors. Moreover, it is not clear what types of electron donors are responsible for

Submitted December 29, 2008, and accepted for publication March 6, 2009.

*Correspondence: esatyy@utu.fi

Editor: Janos K. Lanyi.

0006-3495/09/06/4672/9 $2.00

doi: 10.1016/j.bpj.2009.03.007

the reduction of the Mn cluster during the conversion of S_3 and S_2 to lower S states when the PS II center does not have Q_B^-.

In this study, we aimed to clarify the mechanism of deactivation of the S_3 and S_2 states into lower S states in PS II of thylakoid preparations. For this, we evaluated the kinetics of S state redistribution in thylakoid membranes in the dark after one or two short laser flashes (preflashes). The flash-induced oxygen evolution pattern was measured at various time intervals after the preflash(es) and analyzed with an extended one-miss model that also included slow inactivation of PS II during a prolonged flash sequence. The kinetics of S state redistribution was fitted by a model that assumed that $S_2Q_B^-$ and $S_3Q_B^-$ decay to S_1Q_B and S_2Q_B, respectively. Two mechanisms were tested for the decay of S_2Q_B and S_3Q_B. The first one is represented by successive one-electron-per-step decay of S_3Q_B via S_2Q_B to S_1Q_B whereas the second mechanism assumes the two-electron transitions $S_2Q_B \rightarrow S_0Q_B$ and $S_3Q_B \rightarrow S_1Q_B$. The data show that two-electron reactions occur in the absence of chemical additives, whereas the one-electron-per-step mechanism becomes predominant in the presence of electron acceptors, such as 2,6-dichlorobenzoquinone (DCBQ) and dichlorophenol-indophenol (DCPIP). The one-electron-per-step pathway was predominant also in PS II membrane fragment preparations. Water and hydrogen peroxide were examined as possible sources of electrons for the two-electron reactions of deactivation.

MATERIALS AND METHODS

Preparation of thylakoid membranes and membrane fragments enriched in PS II (BBY-particles)

Pumpkin plants were grown at the photosynthetic photon flux density of 150 μmol m^{-2} s^{-1} in a 12-h day/night rhythm. Thylakoids were isolated according to Hakala et al. (21) and stored at −70°C until use. For the experimental treatments, thylakoids (4 mg chlorophyll (Chl) ml^{-1}) were thawed in the dark on ice and suspended in PS II measurement buffer containing 40 mM HEPES-KOH, pH 7.6; 0.33 M sorbitol, 5 mM $MgCl_2$, 5 mM NaCl, 1 M glycine betaine, 1 mM KH_2PO_4, and 5 mM NH_2Cl.

PS II-enriched membrane fragments (BBY-particles) were isolated essentially according to Berthold et al. (22) as follows. Leaves were homogenized in cold buffer containing 50 mM HEPES, pH 7.5, 0.4 M NaCl, 3 mM $MgCl_2$,1 mM EDTA, and 0.2% BSA, and the homogenate was filtered through Miracloth (Calbiochem, Darmstadt, Germany) and centrifuged for 10 min at 200 × g at 4°C. The supernatant was centrifuged for 10 min at 1000 × g and the pellet was suspended in small amount of a second buffer (50 mM HEPES, pH 7.5, 150 mM NaCl, and 4 mM $MgCl_2$), pelleted (10 min 5000 × g) and resuspended in 50 mM MES, pH 6.1, 15 mM NaCl, 5 mM MgCl2, and 1 mM ascorbic acid. The chlorophyll concentration of the homogenate was adjusted to 2 mg/mL, 25% Triton X-100 was added slowly to yield 1:20 Chl/Triton-X ratio (w/w) and the homogenate was incubated for 30 min in darkness on ice under constant stirring. Subsequently, the homogenate was centrifuged for 30 s at 200 × g. The supernatant was centrifuged for 30 min at 30,000 × g, and the pellet was washed twice by centrifugation (30,000 × g, 30 min) in buffer containing 50 mM MES, pH 6.0, 0.4 M sucrose, and 10 mM NaCl. Finally, BBY-particles were resuspended in the same buffer. BBY particles containing 2.5 mg Chl/mL were stored at −70°C.

Measurement of flash-induced O_2 evolution

Flash-induced O_2 evolution was measured with a Joliot-type bare platinum electrode (23). Flashes (4 ns, 12 mJ/pulse, 532 nm) were fired by an Nd/YAG laser (Minilite, Continuum, Santa Clara, CA) at the repetition rate of 1 flash/s. A lens was set over the electrode to defocus the laser beam on a surface of 5 mm^2. The amplified amperometric signals from the oxygen electrode were recorded with a personal computer.

Thylakoid membranes were thawed in the dark on ice and suspended in PS II measurement buffer (0.8 mg Chl/mL). In all measurements, OEC was synchronized to state S_1 with oxidized Y_D ($S_1Y_D^{ox}$ thylakoids) by placing the sample on the electrode and treating it according to the following protocol: 5 min darkness–one flash–10 min darkness–one flash–15 min darkness. Thereafter the polarization voltage (−710 mV) of the oxygen electrode was switched on and one or two preflashes were fired, as indicated in each experiment. Reagents like exogenous electron acceptors were added 3 min before the preflashes, as indicated, and the sample was kept in the dark for a period specific for each experiment. Finally, flash-induced O_2 evolution pattern was measured using a train of 15 flashes. All measurements were done at 22°C.

Evaluation of *S*-state distribution

Flash-induced O_2 evolution was analyzed with a model that is an extension of the classical Kok scheme of oxygen evolution (6). The model assumes that all misses occur during one S-state transition, $S_3 \rightarrow S_0$, and the miss probability was assumed to be zero during all other transitions (one-miss model). The double hit probability was assumed to be zero because one 4-ns flash can only induce one turnover of PS II. The model was also extended to include nonspecific decrease in O_2 evolving activity during the measurement of the flash oxygen sequence; such slow inactivation is frequently observed in subcellular preparations in the absence of artificial electron acceptors (24).

Modeling deactivation of higher *S* states

The kinetics of the deactivation of the S_2 and S_3 states was analyzed assuming that the deactivation of the S_2 and S_3 states in centers with reduced Q_B occurs via reactions of charge recombination: $S_2Q_B^- \rightarrow S_1Q_B$, $S_3Q_B^- \rightarrow S_2Q_B$, whereas states S_2Q_B and S_3Q_B may decay either via a one-electron-per-step route, $S_3Q_B \rightarrow S_2Q_B \rightarrow S_1Q_B$ or via a mixed route involving both one and two-electron reactions, $S_2Q_B \rightarrow S_0Q_B$, $S_2Q_B \rightarrow S_1Q_B$ and $S_3Q_B \rightarrow S_1Q_B$ (Fig. 1). All modeling, including the analysis of the flash-induced oxygen evolution pattern, was done with the ModelMaker 4 software (Cherwell Scientific, Oxford, UK).

Hydrogen peroxide assay

Hydrogen peroxide was quantified using Amplex UltraRed reagent (Invitrogen, Carlsbad, CA), which in the presence of peroxidase reacts with H_2O_2 and produces highly fluorescent resorufin. The excitation and emission maxima of resorufin fluorescence are 576 and 581 nm, respectively. For the assay, a thylakoid sample was first treated with flashes as indicated for each experiment. Then, horseradish peroxidase (1 μM) and Amplex UltraRed (5 μM) were added to 100 μL of the thylakoid sample, and the sample was incubated for 10 min in the dark to allow the deactivation of the higher S states to occur. The sample was then centrifuged at 22,000 × g for 8 min at 4°C to remove thylakoids. Fifty microliters of supernatant was diluted by 450 μL of 40 mM HEPES (pH 7.6). Resorufin fluorescence was excited with a KL-1500 light source (Schott, Mainz, Germany) through a 550 nm short-pass filter (Corion, Newport Corporation, Franklin, MA). Fluorescence emission was measured with an Ocean Optics S2000 spectrometer through a high-pass 600 nm cutoff filter (Corion). The height of the emission peak at 600 nm, precalibrated versus H_2O_2 concentration, was used to quantify H_2O_2 from the samples. All measurements were carried out in darkness or in dim green light.

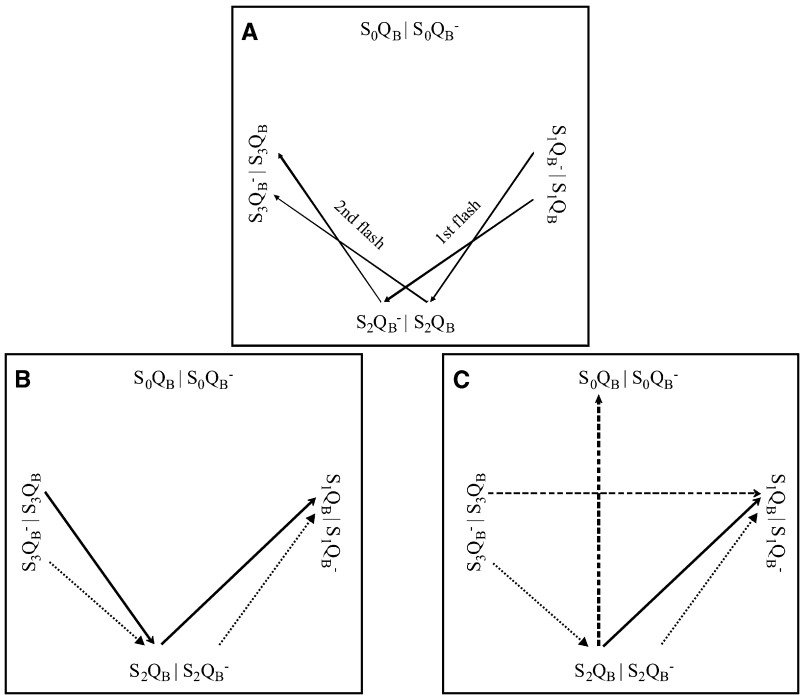

FIGURE 1 Scheme of *S* state transitions induced by one or two preflashes (*A*) and transitions occurring during consequent dark deactivation in PS II centers according to the classical one-electron-per-step mechanism (*B*) and according to the proposed two-electron mechanism (*C*). Before the preflashes were fired, all PS II centers were assumed to be in the $S_1Y_D^{ox}$ state with 20% Q_B^- and 80% Q_B. In *B* and *C*, one-electron and two-electron reactions occurring during deactivation of states S_2Q_B and S_3Q_B are shown with solid and dashed arrows, respectively, and charge recombination of pairs $S_2Q_B^-$ and $S_3Q_B^-$ is indicated by dotted arrows.

Measurement of delayed light emission

Delayed light emission was measured at 20°C with a home-made luminometer described earlier (25). In this experiment, all flash treatments were done with a FX-200 Xenon flash lamp using the flash energy of 1 J.

RESULTS AND DISCUSSION

Analysis of flash-induced O_2 evolution

The modeling of the changes in *S* state populations occurring during dark incubation after one or two preflashes (Fig. 1) was based on analysis of flash-induced O_2 evolution patterns. Assumptions about the miss parameter are crucial for this analysis. In the classical Kok scheme, the probability of misses is assumed to be equal for each *S* state transition (6). This model shows good fit to experimental data when double hits are assumed to occur. Double hits reflect actual double turnovers of OEC during a ''long'' (μs range) flash from a Xenon lamp, and the use of shorter flashes diminishes double hits (26). In our experiments, the probability of double hits was zero because 4-ns laser flashes are too short to induce double turnovers. However, omission of double hits makes the model for the flash oxygen sequence simpler and therefore less flexible than models containing double hits (27). Because of the reduced flexibility, we found it no longer possible to fit the oxygen sequences if the miss probability was the same for all *S* states. Therefore, we tested more complex models, assuming that the miss probability is different for each *S* state transition (9,10).

From the viewpoint of modeling, the assumption that the miss probability is unequal is problematic, because unequal miss probabilities make the oxygen sequence underdetermined (28) and therefore the same sequence can be fitted with several different distributions of the miss probability. However, direct estimation of the miss probability of each *S* state transition with EPR spectroscopy has given strong evidence recently favoring the idea that the miss probability is different for different *S* state transitions (G. Han, S. Styring, F. Mamedov, Uppsala University, Sweden, personal communication, 2008). In our modeling, we tested various models with unequal miss probabilities, and the best fit was obtained when all misses were assumed to occur during one specific *S* state transition, whereas the miss probabilities of all other transitions were set to zero (one-miss model (9)). Models assuming that the miss occurs during $S_0 \rightarrow S_1$, $S_1 \rightarrow S_2$, $S_2 \rightarrow S_3$, or $S_3 \rightarrow S_0$ showed the same goodness of fit but predicted different initial distributions of the *S* states (Table 1). The option that the miss occurs during the $S_0 \rightarrow S_1$ transition was excluded because this model predicted an unrealistic initial population of *S* states (Table 1). The three other models predicted that ~95% of OEC was initially in the S_1 state in dark-adapted $S_1Y_D^{ox}$ thylakoids, and we chose to assume that the miss occurs during the $S_3 \rightarrow S_0$ transition. The assumption excludes misses during illumination of a dark-adapted sample by one or two flashes. A typical flash-induced O_2 evolution pattern measured from $S_1Y_D^{ox}$ thylakoids after two preflashes followed by a 10-min dark adaptation is shown in Fig. 2 (*curve 2*) together with the fit obtained with the one-miss model.

O_2 evolution declined with the number of flashes fired (Fig. 2, *inset*). A similar decline has been observed frequently in the absence of electron acceptors (24). In our case, the decline was strongly diminished in the presence of 1 mM potassium hexacyanoferrate(III) (FeCy) (Fig. 2,

TABLE 1 Parameters calculated by fitting flash-induced O_2 evolution pattern recorded in $S_1Y_D^{ox}$ thylakoid preparations by using the one-miss model that assumes that all misses occur during one specific *S* state transition, $S_1 \rightarrow S_2$, $S_2 \rightarrow S_3$, $S_3 \rightarrow S_0$, or $S_0 \rightarrow S_1$

	S-state transition at which all misses occur			
Model parameter	$S_1 \rightarrow S_2$	$S_2 \rightarrow S_3$	$S_3 \rightarrow S_0$	$S_0 \rightarrow S_1$
S_0 (initial), %	3.5	3.2	3.4	36.8
S_1 (initial), %	95.4	94.9	94.6	61.9
S_2 (initial), %	1.0	1.9	1.7	1.1
S_3 (initial), %	0.1	0.0	0.3	0.2
d (%)*	0.4	0.4	0.4	0.4
Miss probability	0.346	0.346	0.346	0.346
χ^2, $\times 10^{-4\dagger}$	3.7	3.8	3.8	4.1

A typical flash-induced O_2 evolution pattern was used for the analysis.
*Parameter accounting for decrease in O_2 evolution per flash during prolonged flashing.
$^\dagger\chi^2$ evaluates the goodness of the fit.

inset) and the decline could also be reversed in the dark (data not shown). These data indicate that O_2 evolution declines because repetitive flashing reduces the electron acceptor quinones of PS II. To account for this effect, the model was extended to include flash-induced decrease in O_2 evolution (parameter *d*).

Modeling deactivation of *S* states

The deactivation of higher *S* states can occur via charge recombination between the donor and acceptor sides of PS II ($S_2Q_B^- \rightarrow S_1Q_B$, and $S_3Q_B^- \rightarrow S_2Q_B$) or by oxidation of the reduced tyrosine Y_D by the S_2 or S_3 state (8–10,29). If Y_D is in the oxidized state and recombination between the $S_2(S_3)$ state and Q_B^- is suppressed by using the artificial electron acceptor PPBQ, then the S_3 state decays slowly in two one-electron steps via S_2 (17). To study the deactivation of higher *S* states in the absence of chemical additives, we explored the kinetics of *S* state repopulation in darkness after illumination of $S_1Y_D^{ox}$ thylakoids by one or two flashes. The kinetics was determined in the traditional way by varying the dark-time between firing of flashes and measurement of the flash-induced O_2 evolution pattern. Curve 1 in Fig. 2 shows a flashinduced O_2 evolution pattern measured from $S_1Y_D^{ox}$ thylakoids after two preflashes followed by a short dark adaptation. The patterns were fitted with the one-miss model and deconvoluted into *S* state populations using the models presented in Fig. 1.

The time courses of the distributions of *S* states observed after one and two preflashes are plotted as a function of the dark time in Fig. 3, *A* and *B*, respectively. Two phases were observed in the decay of the higher *S* states. The fast phase coincided kinetically with the decay of delayed light emission after a short flash (Fig. 3 *A*, *inset*), indicating that the fast phase originates from the recombination reactions $S_2Q_B^- \rightarrow S_1Q_B$ (Fig. 3 *A*) and $S_3Q_B^- \rightarrow S_2Q_B$ (Fig. 3 *B*).

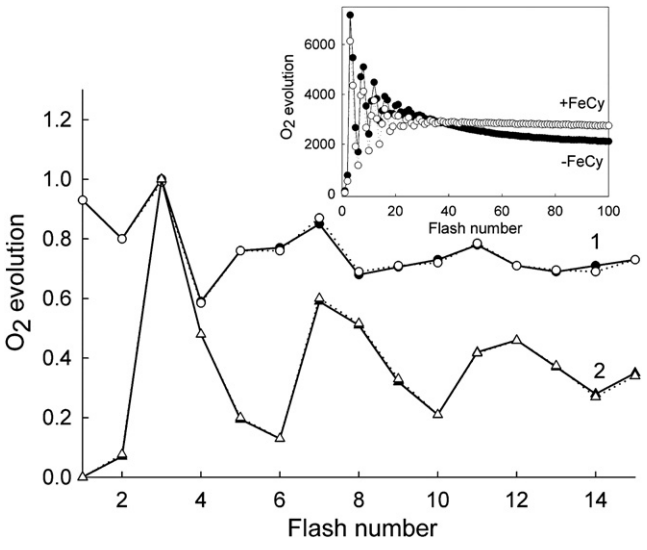

FIGURE 2 Flash-induced O_2 evolution patterns measured in $S_1Y_D^{ox}$ thylakoid preparations (*solid symbols*) and the best fit (*open symbols*) calculated by using the one-miss model with all misses occurring in the $S_3 \rightarrow S_0$ transition. $S_1Y_D^{ox}$ thylakoids were treated with two preflashes, and the O_2 evolution pattern was then measured after 2 (*curve 1*) or 10 (*curve 2*) min of dark incubation. Amplitudes of O_2 evolution are normalized to the maximal value in the train. (*Inset*) Flash-induced O_2 evolution measured under the same conditions as in curve 2 in the presence or absence of 1 mM FeCy, as indicated. The data show typical flash-induced O_2 evolution patterns.

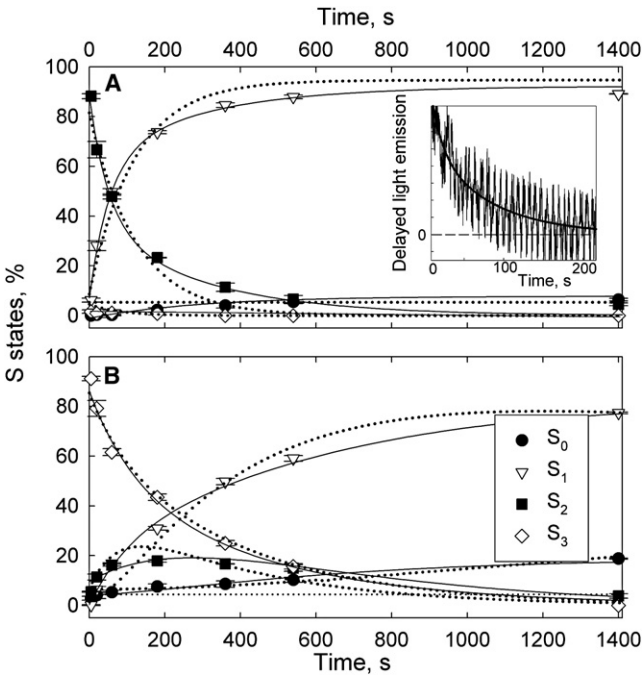

FIGURE 3 Deactivation kinetics of *S*-states after one (*A*) or two (*B*) preflashes in $S_1Y_D^{ox}$ thylakoid membranes. The data show the percentage of the sum of all *S* states: $S_0 + S_1 + S_2 + S_3 = 100\%$. Each data point represents the average of three repeats, and error bars show standard deviation. Fitting was done using the one-electron-per-step model for the deactivation of the higher *S*-states (*dotted lines*, the model is shown in Fig. 1 *B*) and using the two-electrons-per-step model (*solid lines*, the model is shown in Fig. 1 *C*). (*Inset*) Decay of delayed light emission after one flash in $S_1Y_D^{ox}$ thylakoids.

TABLE 2 Effects of oxidizing and reducing agents on half-times of the indicated reactions of deactivation and on the relative amplitude of the one-electron reaction $S_3 \rightarrow S_2$

	$\tau_{1/2}$, s					
Chemical addition	$S_3Q_B \rightarrow S_1Q_B$	$S_2Q_B \rightarrow S_1Q_B$	$S_2Q_B \rightarrow S_0Q_B$	$S_1Q_B \rightarrow S_0Q_B$	Amplitude of $S_3 \rightarrow S_2$(%)	χ^2
None (control)	230	860	1380	nd	25	2.23
250 μM DCPIP	109	128	nd	6.3×10^3	52	1.10
250 μM DCPIP, 1 mM ascorbate	116	142	nd	4.8×10^3	49	2.46
250 μM DCBQ	61	105	nd	4.0×10^3	77	6.78
250 μM DCBQ, 1 mM FeCy	58	123	nd	7.1×10^3	71	4.56
1 mM FeCy	128	209	nd	8.6×10^4	48	5.23
1 mM ascorbate	173	288	nd	3.4×10^4	43	3.14
BBY particles, no additions	49	115	nd	nd	65	11.8

Deactivation was induced by firing two flashes on $S_1Y_D^{ox}$ thylakoid membranes. Where indicated, kinetics was measured and analyzed in BBY particles under the same conditions. Reagents were added 3 min before the two preflashes were fired. The half-times were calculated from the kinetics of the S_3 state deactivation by using the model in Fig. 1 *B* extended with the reaction $S_1Q_B \rightarrow S_0Q_B$. The half-time of the recombination reaction $S_3Q_B^- \rightarrow S_2Q_B$ (52 s) was assumed to be independent of the chemical additions. The relative amplitude of the $S_3 \rightarrow S_2$ component was calculated as the ratio of the amplitude of the $S_3 \rightarrow S_2$ component to the sum of the amplitudes of the $S_3 \rightarrow S_2$ and $S_3 \rightarrow S_1$ components. Goodness of the fit was evaluated with χ^2; nd = not detected.

The slow phase, in turn, can be attributed to deactivation of the S_2Q_B and S_3Q_B states that lack an apparent electron donor to S_2 and S_3. The initial amount of the S_1 state in Fig. 3 *A* and the initial amount of the S_2 state in Fig. 3 *B* was ~5%, indicating a minor presence of the S_0 state in $S_1Y_D^{ox}$ thylakoids. The kinetics of the S_2 state observed in the samples illuminated by two flashes (Fig. 3 *B*) showed a fast rise related to recombination between the S_3 state and Q_B^- during the first 50 s, and a slower decline that visually coincides with increase in S_0. The amplitude of the increase in S_0 was larger in samples excited by two preflashes (12%; Fig. 3 *B*) as compared to 3% in preparations excited by one preflash (Fig. 3 *A*), indicating that the amount of the precursor whose deactivation leads to the S_0 state is different after one preflash and after two preflashes.

Deactivation of the higher *S* states in PS II with oxidized Q_B and Y_D can be ascribed to the one-electron-per-step sequence: $S_3Q_B \rightarrow S_2Q_B \rightarrow S_1Q_B$ (Fig. 1 *B*). However, we failed to obtain a satisfactory fit using this one-electron-per-step model (Fig. 3, *dotted lines*), as it required more rapid deactivation of higher *S* states than was observed. Moreover, an increase in the S_0 state was observed after illumination of $S_1Y_D^{ox}$ thylakoids by two flashes (Fig. 3 *B*), and this increase cannot be explained with the one-electron-per-step model that implies deactivation of the S_2 and S_3 states only to the dark stable S_1 state (Fig. 1 *B*) (7,29). The slow rise of the S_0 state cannot be due to the appearance of Y_D^{red} because Y_D^{red} would be rapidly reoxidized by the higher *S* states.

Seibert and Lavorel (20) examined the deactivation of *S* states in PS II preparations in the absence of artificial electron acceptors and found that the decay of the S_2 state seems to be independent of the decay of the S_3 state. We tested the hypothesis that independent routes of deactivation of the S_3 and S_2 states involve the two-electron reactions $S_3Q_B \rightarrow S_1Q_B$ and $S_2Q_B \rightarrow S_0Q_B$ (Fig. 1 *C*). The two-electron mechanism improved the fit significantly for data obtained both after one preflash and after two preflashes (Fig,. 3, *A* and *B*, *solid lines*). Intermediate models including only one two-electron route (either $S_3Q_B \rightarrow S_1Q_B$ or $S_2Q_B \rightarrow S_0Q_B$) showed lower goodness of fit than the model including both routes (data not shown). Thus, five reactions seem to be involved in deactivation of higher *S* states in Y_D^{ox} thylakoids (Fig. 1 *C*). Two of the reactions can be ascribed to charge recombination between the S_2 and S_3 states and Q_B^-, whereas the three other reactions, $S_3Q_B \rightarrow S_1Q_B$, $S_2Q_B \rightarrow S_0Q_B$, and $S_2Q_B \rightarrow S_1Q_B$, occur in PS II with oxidized Q_B. Reactions $S_2Q_B \rightarrow S_0Q_B$ and $S_2Q_B \rightarrow S_1Q_B$ occur both after one and two flashes, suggesting that the same mechanism functions in both cases.

The half-times of the states $S_2Q_B^-$ and $S_3Q_B^-$ were 57 and 52 s, respectively, which is somewhat slower than has been usually observed ($\tau_{1/2}$ = 20–40 s) (8,16). Furthermore, half-times of reactions $S_3Q_B \rightarrow S_1Q_B$, $S_2Q_B \rightarrow S_1Q_B$, and $S_2Q_B \rightarrow S_0Q_B$ were 230, 860, and 1380 s, respectively (Table 2, *control*). In particular, the decay of the S_2Q_B state was slower than reported earlier for the reaction $S_2Q_B \rightarrow S_1Q_B$ ($\tau_{1/2}$ ~ 150–240 s) (16,17).

The ratios between amplitudes of the slow and fast decay components, which reflect the ratios between the initial states of PS II with oxidized and reduced Q_B (Q_B/Q_B^-), were 19:81 and 75:25 for samples illuminated by one and two flashes, respectively. Taking into account that each flash reverses the redox state of Q_B as shown in Fig. 1 *A*, this result indicates that $S_1Y_D^{ox}$ thylakoids contain 20%–25% of PS II centers with Q_B^-.

Effects of artificial electron acceptors on deactivation reactions

Some artificial electron acceptors, including benzoquinone derivatives and DCPIP, may noticeably influence the rate of the deactivation of *S* states, possibly because the reduced forms of the electron acceptors mediate shifts of OEC from more oxidized *S* states toward more reduced *S* states (18,19). Furthermore, in the presence of PPBQ, the S_3Q_B state decays in a one-electron-per-step manner via S_2Q_B

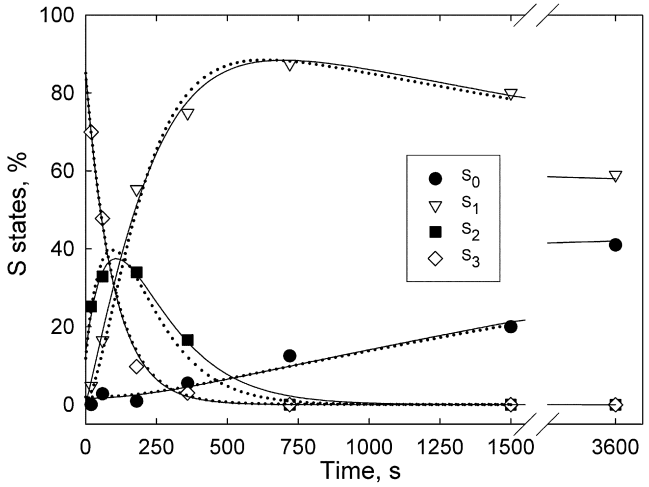

FIGURE 4 Deactivation kinetics of *S* states after two preflashes in $S_1Y_D^{ox}$ thylakoid membranes in the presence of 250 μM DCBQ. The data show the percentage of the sum of all *S*-states: $S_0 + S_1 + S_2 + S_3 = 100\%$. Fitting was done using the one-electron-per-step model for the deactivation of the higher *S* states (*dotted lines*) and using the two-electrons-per-step model (*solid lines*) (see models in Fig. 1 *B* and *C*). Both models were extended by including the reaction $S_1Q_B \rightarrow S_0Q_B$. The kinetic pattern is from one representative experiment.

(17) whereas a two-electron reaction, $S_3Q_B \rightarrow S_1Q_B$, occurs in the absence of additives (see previous section). To clarify the mechanism of deactivation in the presence of artificial electron acceptors, we measured the decay kinetics of the S_3 state in the presence of DCBQ and in the presence of DCPIP. The half-times and amplitudes of the reactions were calculated according to the two-electrons-per-step-model (Fig. 1 *C*). DCBQ is known to mediate a shift from the S_1 to the S_0 state (30) and therefore the model was extended by the reaction $S_1Q_B \rightarrow S_0Q_B$. When 250 μM DCBQ or DCPIP were added, the half times of reactions $S_3Q_B \rightarrow S_1Q_B$ and $S_2Q_B \rightarrow S_1Q_B$ were diminished by 2.0–4.0 and 6.0–8.0 times, respectively, as compared to control measurements done in the absence of chemical additives (Table 2). Furthermore, these reagents completely inhibited the two-electron reaction $S_2Q_B \rightarrow S_0Q_B$, and a new slow one-electron reaction $S_1Q_B \rightarrow S_0Q_B$ appeared with a half time of 4.0–6.3 $\times$ 10^3 s (1.1–1.8 h). DCBQ caused a more pronounced effect than DCPIP (Table 2) and the presence of DCBQ led to increase in S_0 at the expense of S_1. Fig. 4 shows the time-course of the redistribution of the *S* states in darkness after two preflashes in the presence of DCBQ. Furthermore, DCPIP plus ascorbate and DCBQ plus FeCy caused practically the same changes to kinetics as those observed in the presence of oxidized DCPIP or DCBQ alone (Table 2). Ascorbate reduces DCPIP and FeCy would oxidize any reduced hydroquinone form of DCBQ. These data indicate that DCPIP and DCBQ themselves do not act as electron sources to OEC. Moreover, despite the fact that FeCy is a potent oxidizing agent ($E^{o\prime} = 456$ mV at pH 7.0), and ascorbate is a mild reductant, both reagents enhanced the decay of the S_2 and S_3 states (Table 2). However, effects of FeCy and ascorbate were weaker than the effects of DCPIP and DCBQ. These data indicate that the acceleration of the deactivation of the higher *S* states in the presence of redox agents can not be explained by an alteration of the redox conditions within the electron transport chain.

In control thylakoids, the one-electron-per-step route of the decay of the S_3 state ($S_3 \rightarrow S_2$) is attributed to the charge recombination $S_3Q_B^- \rightarrow S_2Q_B$, and ~25% of the S_3 state was deactivated via this pathway in control thylakoids (Table 2). The amplitude of the one-electron-per-step component of the decay of S_3 increased to 50% in the presence of DCPIP and to 70%–80% in the presence of DCBQ (Table 2). Furthermore, the rate of the deactivation of S_3 was fastest in the presence of DCBQ and DCPIP, intermediate in the presence of FeCy and ascorbate, and slowest in the control.

The increase in the amplitude of the fast component of S_3 decay in the presence of the combination of DCPIP and ascorbate (Table 2) that efficiently reduces the plastoquinone pool (31), may be caused by recombination reactions between the higher *S* states and the quinone electron acceptors. Ascorbate alone causes a similar but weaker effect (Table 2), as expected because ascorbate only weakly interacts with the plastoquinone pool (32). However, both DCPIP and DCBQ would rather oxidize than reduce Q_B, suggesting that in the presence of these electron acceptors, the main substrate of the fast component is S_3Q_B, not $S_3Q_B^-$. Interestingly, the deactivation of the higher *S* states, measured in the presence of 250 μM DCBQ, could be fitted with the one-electron-per-step model of deactivation (Fig. 4, *dotted lines*). We suggest that DCBQ and oxidized DCPIP disturb OEC in such a way that the one-electron reactions $S_3Q_B \rightarrow S_2Q_B$ and $S_2Q_B \rightarrow S_1Q_B$ occur instead of the slow two-electron reaction $S_3Q_B \rightarrow S_1Q_B$. The accelerating effect of the oxidants on the decay of the S_3 state decreased with decreasing lipophilicity: DCBQ (lipophilic) > oxidized DCPIP (soluble in both water and organic solvents) > FeCy (hydrophilic), suggesting that lipophilicity of the reagent is more important than oxidizing power. We propose that the lipophilic reagents have more direct access to PS II, and, hence, may cause chemical disturbance of OEC. The exact nature of the disturbance is unknown, but possibly these chemicals modify the protein envelope at the donor side of PS II making inner part of OEC more accessible to nonspecific external reductants.

We also tested deactivation reactions in BBY particles in the absence of electron acceptors. In these preparations, the miss factor and the inactivation parameter *d* had high values. The value of *d* apparently reflects a smaller number of (oxidized) plastoquinone per PS II in the BBY particles than in thylakoid membranes; this also leads to recombination between P_{680}^+ and Q_A^-, and, hence, contributes to the high miss factor. Due to the high and somewhat varying values of these two parameters, the goodness of the fit of the

O_2 evolution sequence, estimated with χ^2, was much lower in BBY particles than in thylakoids (Table 2). Deactivation of the S_3 state occurred faster and the contribution of the two-electron reactions was smaller in BBY particles than in thylakoids (Table 2). Deactivation of S_3 in BBY particles actually resembles the kinetics observed in thylakoids in the presence of DCBQ, except that the reaction $S_1Q_B \rightarrow S_0Q_B$ did not occur in BBYs. These data may suggest that detergents used in the preparation of BBY particles cause similar disturbance of OEC as DCBQ and DCPIP.

Testing hydrogen peroxide and water as electron donors for the two-electron deactivation reactions

Two-electron reactions dominate the deactivation kinetics of higher S states in PS II with oxidized Q_B and Y_D (Fig. 3, Table 2). Hypothetically, hydrogen peroxide can act as an electron donor for the reaction $S_2Q_B \rightarrow S_0Q_B$. We also tested the thermodynamically unfavorable possibility that water would be oxidized in the reaction $S_3Q_B \rightarrow S_1Q_B$. It has been shown earlier that OEC in the S_2 state can oxidize H_2O_2 with the subsequent formation of the S_0 state and molecular oxygen (33). If water was the electron donor in reaction $S_3Q_B \rightarrow S_1Q_B$, then the slow oxidation of H_2O would be accompanied with the formation of a peroxo-Mn-complex, and this step would be followed by the exchange of hydrogen peroxide to water. Two-electron oxidation of water (E_h at pH 7 = 1.362 V) would require more energy than four-electron reaction (E_h at pH 7 = 0.815 V) (see also Bendall and Sofrová (34)), and therefore two-electron oxidation of water would have a very slow rate. This is in agreement with our data, as the reaction $S_3Q_B \rightarrow S_1Q_B$ was characterized by a time constant of several minutes (Table 2, *control*).

If H_2O_2 acts as an electron donor in a two-electron deactivation reaction, then this reaction would decrease the H_2O_2 concentration. Two-electron oxidation of water, in turn, would increase the concentration H_2O_2. To test these assumptions, we measured the concentration of H_2O_2 in isolated thylakoids during the deactivation of the higher S states. In the light, generation of H_2O_2 occurs mainly via reduction of oxygen by the reduced electron acceptors of PS I. PS II is also known to produce H_2O_2, probably by a reaction between plastosemiquinone and oxygen (35). H_2O_2 is decomposed in thylakoid preparations by internal catalase-like activity and by catalase that is present as an impurity. We used the Amplex UltraRed/horseradish peroxidase system to measure changes in the H_2O_2 concentration of a thylakoid sample during 10 min of dark incubation. Analysis of resorufin fluorescence showed that thylakoid membranes generated ~0.3 molecule of H_2O_2 per one PS II center during the 10 min incubation (Fig. 5 *A*). Similar incubation carried out under an argon flow diminished production of H_2O_2 by 70%–80%, equally as much as did the addition of catalase, indicating that the major part of the signal originates from the reduction of oxygen. To measure the total production of H_2O_2, thylakoids were first incubated for 1 min with 5 mM sodium azide to suppress their catalase activity, washed once with a fresh buffer, and incubated for 10 min with Amplex Ultrared and peroxidase. These preparations showed 50% more H_2O_2 production as compared with untreated thylakoids (Fig. 5 *A*). These data indicate that H_2O_2 is generated spontaneously in thylakoids, probably because of interactions between oxygen and reduced forms of photosynthetic electron carriers.

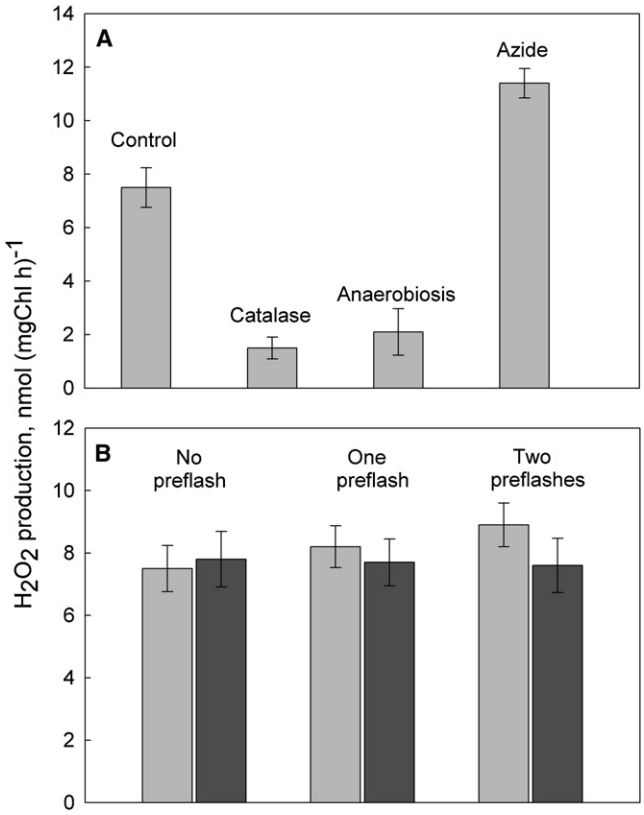

FIGURE 5 Production of hydrogen peroxide in thylakoids during 10 min dark incubation under different conditions. (*A*) Production of H_2O_2 in dark-adapted $S_1Y_D^{ox}$ thylakoids incubated without additives (control), with catalase (30 U in 100 μL), under argon flow, and after treatment with 5 mM sodium azide. (*B*) Production of H_2O_2 in $S_1Y_D^{ox}$ thylakoids during 10 min dark incubation of nonilluminated samples and after illumination of the sample with one or two flashes as indicated. The measurements were carried out in the presence (*dark gray*) or absence (*light gray*) of 0.4 μM CCCP, added 10 s after the preflash(es) were fired. H_2O_2 was measured with the Amplex Ultrared method. Each bar represents an average of three independent experiments and the error bars show standard deviation.

To find out whether the deactivation process influences the H_2O_2 content, we measured H_2O_2 production after illumination of $S_1Y_D^{ox}$ thylakoids by one or two flashes. The assay reagents, Amplex UltraRed and peroxidase, were added into the sample 20 s after firing the flash(es), and the mixture was incubated for 10 min in the dark before the fluorescence signal was measured. CCCP, which is an ADRY reagent (acceleration of the deactivation reactions of the water-splitting enzyme

system Y), was used to speed up reactions of deactivation so that they were completed before the addition of the H_2O_2 assay reagents (36). As shown in Fig. 5 *B*, CCCP did not affect production of H_2O_2 in dark-adapted thylakoids, whereas slightly less (statistically not fully resolved) H_2O_2 was produced in the presence of this reagent in preparations illuminated by one or two flashes. These data show that a small amount of hydrogen peroxide, corresponding to one molecule per 20–30 PS II centers, is probably generated during the deactivation process. However, the amplitude of the $S_3Q_B \rightarrow S_1Q_B$ component was ~75% and therefore the amount H_2O_2 produced would be higher by one order of magnitude than the observed amount if water was the electron donor in the deactivation of S_3Q_B. Thus, we conclude that water does not act as an electron donor to the $S_3Q_B \rightarrow S_1Q_B$ reaction. These data also indicate that internally produced H_2O_2 does not act as an electron donor to this reaction, because no decrease in H_2O_2 production was observed in thylakoids after illumination by two flashes.

The reaction $S_2Q_B \rightarrow S_0Q_B$ is slow ($\tau_{1/2} = 23$ min) and has a low amplitude (12%), which makes it difficult to directly measure the decrease in H_2O_2 associated with this reaction. Therefore, we measured the kinetics of the S_3 state deactivation in the presence of catalase, which decreases the amount of the internally produced H_2O_2 (Fig. 5 *A*) and, hence, should slow down reaction $S_2Q_B \rightarrow S_0Q_B$ if the latter reaction is coupled to oxidation of H_2O_2. The reaction $S_2Q_B \rightarrow S_0Q_B$ was slightly slower in the presence of catalase ($\tau_{1/2} = 1540$ s), as compared to control ($\tau_{1/2} = 1380$ s), and its amplitude was 5%, that is <12% amplitude in control thylakoids. The catalase treatment had virtually no effect on the other kinetic components (data not shown). Due to the low amplitude of the reaction $S_2Q_B \rightarrow S_0Q_B$ (12%), the changes observed in the presence of catalase are not statistically significant. External H_2O_2 added in concentration of 100 μM into thylakoids did not affect the decay kinetics of the *S* states and 500 μM H_2O_2 caused noticeable changes in the shape of the O_2 evolution pattern accompanied by decrease in O_2 evolution, suggesting damage to OEC (data not shown). These data may indicate that H_2O_2 is not an efficient electron donor to the reaction $S_2Q_B \rightarrow S_0Q_B$ or that external H_2O_2 cannot reach the manganese cluster. The catalase effect may suggest that small amount of hydrogen peroxide produced in thylakoids acts as an electron source for the reaction $S_2Q_B \rightarrow S_0Q_B$. However, more experiments are needed to elucidate the possible role of internally produced H_2O_2 in deactivation of OEC.

CONCLUSION

The deactivation of the higher *S* states of the OEC, particularly of the S_3 state, cannot be entirely explained by the recombination between the donor side of PS II and Q_B^-. The deactivation process has been studied in a number of publications (11,12,13,15), but the slow decay of the S_3 and S_2 states observed in PS II centers with oxidized Q_B is poorly understood. To elucidate the mechanism of the slow deactivation, we measured and analyzed the kinetics of the redistribution of *S* states after illumination of $S_1Y_D^{ox}$ thylakoids by one or two laser flashes. The fast components of the decay of the higher *S* states ($\tau_{1/2} \sim 50$ s) were attributed to recombination between S_2 and S_3 and Q_B^-, whereas the slow components ($\tau_{1/2} > 4$ min) were assigned to the deactivation of S_2 and S_3 in PS II centers containing an oxidized Q_B. The slow components were represented by the one-electron reaction $S_2Q_B \rightarrow S_1Q_B$ ($\tau_{1/2} = 14$ min) and by the two-electron reactions $S_3Q_B \rightarrow S_1Q_B$ ($\tau_{1/2} = 4$ min) and $S_2Q_B \rightarrow S_0Q_B$ ($\tau_{1/2} = 23$ min), reported for the first time in this study. In the presence of artificial electron acceptors, particularly the lipophilic DCBQ, the two-electron reactions were substituted by a more rapid one-electron-per-step sequence, $S_3Q_B \rightarrow S_2Q_B \rightarrow S_1Q_B \rightarrow S_0Q_B$. The deactivation of higher *S* states proceeded predominately via a one-electron mechanism also in BBY particles. Our data suggest that the sensitivity of the deactivation mechanism to the artificial electron acceptors and to the detergents required for extraction of BBY particles may explain why the two-electron reactions were not seen in earlier studies. We suggest that the mechanism of deactivation of the higher *S* states observed in intact thylakoids in the absence of redox reagents characterizes the behavior of OEC in vivo.

Hydrogen peroxide and water were tested as sources of electrons for the two-electron reactions of deactivation. The data suggest that H_2O_2 produced by thylakoids in the dark may to some extent act as a substrate for the slow $S_2Q_B \rightarrow S_0Q_B$ reaction. H_2O_2 assays did not support the hypothesis that water or hydrogen peroxide act as electron donors for the reaction $S_3Q_B \rightarrow S_1Q_B$.

The authors thank Dr. Marja Hakala for ideas and for assistance in experiments.

This study was supported by the Academy of Finland (119557 and 110409).

REFERENCES

1. Goussias, C., A. Boussac, and A. W. Rutherford. 2002. Photosystem II and photosynthetic oxidation of water: an overview. *Philos. Trans. R. Soc. Lond. B Biol. Sci.* 357:1369–1381.
2. Kern, J., and G. Renger. 2007. Photosystem II: Structure and mechanism of the water: plastoquinone oxidoreductase. *Photosynth. Res.* 94:183–202.
3. Ferreira, K. N., T. M. Iverson, K. Maghlaoui, J. Barber, and S. Iwata. 2004. Architecture of the photosynthetic oxygen-evolving center. *Science*. 303:1831–1838.
4. Yano, J., and V. K. Yachandra. 2008. Where water is oxidized to dioxygen: structure of the photosynthetic Mn_4Ca cluster from X-ray spectroscopy. *Inorg. Chem.* 47:1711–1726.
5. Barber, J. 2008. Crystal structure of the oxygen-evolving complex of photosystem II. *Inorg. Chem.* 47:1700–1710.
6. Kok, B., B. Forbush, and M. McGloin. 1970. Cooperation of charges in photosynthetic O_2 evolution. *Photochem. Photobiol.* 11:457–476.
7. Joliot, P., and B. Kok. 1975. Oxygen evolution in photosynthesis. *In* Bioenergetics of Photosynthesis. Govinjee., editor. Academic Press, New York. 388–413.

8. Forbush, B., B. Kok, and M. McGloin. 1971. Cooperation of charges in photosynthetic oxygen evolution-II. Damping of flash yield oscillation, deactivation. *Photochem. Photobiol.* 14:307–321.
9. Delrieu, M. J. 1974. Simple explanation of the misses in the cooperation of charges in photosynthetic oxygen evolution. *Photochem. Photobiol.* 20:441–454.
10. Delrieu, M. J. 1983. Evidence for unequal misses in oxygen flash yield sequence in photosynthesis. *Z. Naturforsch.* 38c:247–258.
11. Babcock, G. T., and K. Sauer. 1973. Electron paramagnetic resonance signal in spinach chloroplasts. I. Kinetic analysis for untreated chloroplasts. *Biochim. Biophys. Acta.* 325:483–503.
12. Rutherford, A. W., A. R. Crofts, and I. Inoue. 1982. Thermoluminescence as a probe of Photosystem II photochemistry: the origin of the flash induced glow peaks. *Biochim. Biophys. Acta.* 682: 457–465.
13. Vass, I., and S. Styring. 1991. pH-dependent charge equilibria between tyrosine-D and the S-states in Photosystem II. Estimation of relative midpoint redox potentials. *Biochemistry.* 30:830–839.
14. Buser, C. A., B. A. Diner, and G. W. Brudvig. 1992. Photooxidation of cytochrome b_{559} in oxygen-evolving photosystem. *Biochemistry.* 31:11449–11459.
15. Feyziyev, Y., B. J. van Rotterdam, G. Bernát, and S. Styring. 2003. Electron transfer from cytochrome b_{559} and tyrosine D to the S_2 and S_3 states of the water oxidizing complex in Photosystem II. *Chem. Phys.* 294:415–431.
16. Rutherford, Govinjee, A. W., and Y. Inoue. 1984. Charge accumulation and photochemistry in leaves studied by thermoluminescence and delayed light emission. *Proc. Natl. Acad. Sci. USA.* 81:1107–1111.
17. Styring, S., and A. W. Rutherford. 1988. Deactivation kinetics and temperature dependence of the S-state transitions in the oxygen-evolving system of Photosystem II measured by EPR spectroscopy. *Biochim. Biophys. Acta.* 933:378–387.
18. Maslenkova, L., and Y. Zeinalov. 1995. Effect of some artificial electron donors and acceptors on the functioning of the photosynthetic oxygen evolving system. *Bulg. J. Plant Physiol.* 21:3–11.
19. Spiegel, S., and K. Bader. 2003. Dependence of the flash-induced oxygen evolution pattern on the chemically and far red light-modulated redox conditions in cyanobacterial photosynthetic electron transport. *Z. Naturforsch.* 58c:93–102.
20. Seibert, M., and J. Lavorel. 1983. Oxygen evolution patterns from spinach Photosystem II preparations. *Biochim. Biophys. Acta.* 723:160–168.
21. Hakala, M., I. Tuominen, M. Keränen, T. Tyystjärvi, and E. Tyystjärvi. 2005. Evidence for the role of the oxygen-evolving manganese complex in photo inhibition of Photosystem II. *Biochim. Biophys. Acta.* 1706: 68–80.
22. Berthold, D. A., G. T. Babcock, and C. F. Yokum. 1981. A highly resolved, oxygen-evolving photosystem II preparation from spinach thylakoid membranes. *FEBS Lett.* 134:231–234.
23. Joliot, P., and A. Joliot. 1968. A polarographic method for detection of oxygen production and reduction of Hill reagent by isolated chloroplasts. *Biochim. Biophys. Acta.* 153:625–631.
24. Delrieu, M. J., and F. Rosengard. 1987. Fundamental difference between period-4 oscillations of the oxygen and fluorescence yield induced by flash excitation in inside-out thylakoids. *Biochim. Biophys. Acta.* 892:163–171.
25. Tyystjärvi, E., S. Rantamäki, and J. Tyystjärvi. 2009. Connectivity of Photosystem II is the physical basis of retrapping in photosynthetic thermoluminescence. *Biophys. J.* 96:3735–3743.
26. Jursinic, P. 1981. Investigation of double turnovers in photosystem II charge separation and oxygen evolution with excitation flashes of different duration. *Biochim. Biophys. Acta.* 635:38–52.
27. Shinkarev, V. P. 2005. Flash-induced oxygen evolution and other oscillation processes. *In* Photosystem II. In Photosystem II: The Water/Plastoquinone Oxido-Reductase In Photosynthesis. T. Wydzynski and K. Satoh, editors. Kluwer Academic Publishers, Dordrecht.
28. Lavorel, J. 1976. Matrix analysis of the oxygen evolving system of photosynthesis. *J. Theor. Biol.* 57:171–185.
29. Velthuys, B. R., and J. W. M. Visser. 1975. The reactivation of EPR signal II in chloroplasts treated with reduced dichlorophenol-indophenol: evidence against a dark equilibrium between two oxidation states of the oxygen evolving system. *FEBS Lett.* 55:109–112.
30. Stemler, A., and J. Lavergne. 1997. Evidence that formate destabilizes the S_1 state of the oxygen-evolving mechanism in photosystem II. *Photosynth. Res.* 51:83–92.
31. Allen, J. F., and N. G. Holmes. 1986. Electron transport and redox titration. *In* Photosynthesis-Energy Transduction. A Practical Approach. M. F. Hipkins and N. R. Baker, editors. IRL Press, Oxford, pp. 103–141.
32. Mano, J., É Hideg, and K. Asada. 2004. Ascorbate in thylakoid lumen functions as an alternative donor to photosystem II and photosystem I. *Arch. Biochem. Biophys.* 429:71–80.
33. Velthuys, B., and B. Kok. 1978. Photosynthetic oxygen evolution from hydrogen peroxide. *Biochim. Biophys. Acta.* 502:211–221.
34. Bendall, D. S., and D. Sofrová. 1971. Reactions at 77°K in Photosystem 2 of green plants. *Biochim. Biophys. Acta.* 234:371–380.
35. Ivanov, B. N. 2008. Cooperation of photosystem I with the plastoquinone pool in oxygen reduction in higher plant chloroplasts. *Biochemistry (Mosc.).* 73:112–118.
36. Renger, G., B. Bouges-Bocquet, and R. Delosme. 1973. Studies on the ADRY agent-induced mechanism of the discharge of the holes trapped in the photosynthetic watersplitting enzyme system Y. *Biochim. Biophys. Acta.* 292:796–807.